

A dessin on the base: a description of mutually non-local 7-branes without using branch cuts

Shin Fukuchi*, Naoto Kan†, Shun'ya Mizoguchi‡ and Hitomi Tashiro§

‡*Theory Center, Institute of Particle and Nuclear Studies, KEK*

Tsukuba, Ibaraki, 305-0801, Japan and

*†‡§*SOKENDAI (The Graduate University for Advanced Studies)*

Tsukuba, Ibaraki, 305-0801, Japan

(Dated: October 12, 2019)

Abstract

We consider the special roles of the zero loci of the Weierstrass invariants $g_2(\tau(z))$, $g_3(\tau(z))$ in F-theory on an elliptic fibration over \mathbb{P}^1 or a further fibration thereof. They are defined as the zero loci of the coefficient functions $f(z)$ and $g(z)$ of a Weierstrass equation. They are thought of as complex co-dimension one objects and correspond to the two kinds of critical points of a dessin d'enfant of Grothendieck. The \mathbb{P}^1 base is divided into several cell regions bounded by some domain walls extending from these planes and D-branes, on which the imaginary part of the J -function vanishes. This amounts to drawing a dessin with a canonical triangulation. We show that the dessin provides a new way of keeping track of mutual non-localness among 7-branes without employing unphysical branch cuts or their base point. With the dessin we can see that weak- and strong-coupling regions coexist and are located across an S -wall from each other. We also present a simple method for computing a monodromy matrix for an arbitrary path by tracing the walls it goes through.

* E-mail: fshin@post.kek.jp

† E-mail: naotok@post.kek.jp

‡ E-mail: mizoguch@post.kek.jp

§ E-mail: tashiro@post.kek.jp

I. INTRODUCTION

The importance of F-theory [1–3] in modern particle physics model building cannot be too much emphasized. The $SU(5)$ GUT, which can naturally explain the apparently complicated assignment of hypercharges to quarks and leptons, is readily achieved in F-theory. Another virtue of F-theory is that it can yield matter in the spinor representation of $SO(10)$, into which all the quarks and leptons of a single generation are successfully incorporated, and which cannot be achieved in pure D-brane models. These features are shared by $E_8 \times E_8$ heterotic models, but F-theory models have an advantage in that they may evade the issue of the relation between the GUT and Planck scales in heterotic string theory first addressed in [4]. Also, the Yukawa couplings perturbatively forbidden in D-brane models [5, 6] can be successfully generated in F-theory.

Almost ten years after the first development in F-theory, there was much progress in the studies of local models of F-theory (See [7–16] for an incomplete list.). In this class of theories, one basically considers a supersymmetric gauge theory¹ on a stack of 7-branes in F-theory, whose coalescence is supposed to give rise to a gauge symmetry depending on the fiber type in the Kodaira classification. In particular, if the fiber type is either IV^* , III^* or II^* , the gauge symmetry will be E_6 , E_7 or E_8 , respectively, and then the brane was called an exceptional brane [8].²

The fiber type of such a codimension-one singularity can be labeled by the (conjugacy class of the) $SL(2, \mathbb{Z})$ monodromy around the fiber. It was shown that all the types of Kodaira fibers can be represented by some product of monodromies of a basic set of 7-branes: \mathbf{A} =D-brane, \mathbf{B} =(1, 1)-brane and \mathbf{C} =(1, -1)-brane [51–53], as shown in Table in Appendix³. The relation between the resolution of the singularity and the gauge symmetry on a coalescence of 7-branes has been clearly explained by using string junctions. String junctions are also useful to describe chiral matter [55], non-simply-laced Lie algebras [56], the

¹ More precisely, the compact part of the theory is “twisted” so that the Casimirs of the gauge fields correctly transform as sections of Looijenga’s weighted projective space bundle [17].

² More recently, after the LHC run in particular, global F-theory models have been attracting much interest. For recent works on global F-theory models, see e.g. [18–50].

³ In this paper, we identify these 7-branes as the monodromy matrices $M_{p,q}$ defined in [51] with the sign of q reversed (as we have adopted Schwarz’s convention for the tension [54]), which are the *inverse* of $K_{[p,q]}$ in [52, 53]; this is consistent as the orderings of the branes and $K_{[p,q]}$ ’s are in reverse to each other.

Mordell-Weil lattice of a rational elliptic surface [57] and deformations of algebraic varieties [58, 59].

From the table one can see that the singular fibers of the exceptional type consist of a **B**-brane and two **C**-branes in addition to the ordinary $D(=\mathbf{A})$ -branes. Thus, in this algebraic approach, the exceptional branes are seen to emerge due to the coalescence of these **B**- and **C**-branes which are distinct from D-branes. From a geometrical point of view, however, these branes are just the zero loci of the discriminant of a Weierstrass equation and there are no a priori differences from each other; they all are locally D-branes.

In this paper, we consider the special roles of the zero loci of the Weierstrass invariants $g_2(\tau(z))$, $g_3(\tau(z))$ in F-theory on an elliptic fibration over \mathbb{P}^1 , or a further fibration thereof. They are defined as the zero loci of the coefficient functions $f(z)$ and $g(z)$ of a Weierstrass equation. They are thought of as complex co-dimension one objects, and we call them “*elliptic point planes*”.

In fact, mathematically, our construction amounts to drawing a “dessin d’enfant” of Grothendieck on the \mathbb{P}^1 base with a canonical triangulation⁴. We show that this drawing provides a new way of keeping track of mutual non-localness among 7-branes in place of the conventional **ABC** 7-brane description. In our approach, all the discriminant loci are treated democratically, and with this “dessin” we can see that weak- and strong-coupling regions coexist and are located across an S -wall from each other. We also present a simple method for computing a monodromy matrix for an arbitrary path by tracing the walls it goes through. The method for studying monodromies by tracing the contours on the $J(\tau)$ -plane was developed long time ago by Tani [55].

This paper is organized as follows: In section 2, we introduce the basic setup of this paper, including the motivations and definitions of the elliptic point planes, the domain walls extended from them, and the cell region decomposition of the \mathbb{P}^1 base of the elliptic fibration. The various definitions of the new notions and objects are summarized as a mini-glossary at the end of this section. In section 3, we briefly explain what is a “dessin d’enfant” and the relation to our present construction. In section 4, we discuss the basic properties of the two kinds of elliptic point planes, the f -plane and the g -plane. In section 5, we present a new method for computing the monodromy by drawing the dessin. In the final section we

⁴ We thank the anonymous referee of Physical Review D for informing us of this fact.

conclude with a summary of our findings. Appendix A contains a table of fiber types of the Kodaira classification. The plots presented in this paper have been generated with the aid of Mathematica.

II. WHAT IS AN ELLIPTIC POINT PLANE?

Consider a Weierstrass equation

$$y^2 = x^3 + fx + g, \tag{1}$$

where y , x , f and g are sections of an $\mathcal{O}(3)$, an $\mathcal{O}(2)$, an $\mathcal{O}(4)$ and an $\mathcal{O}(6)$ bundle over the base \mathbb{P}^1 . This is a rational elliptic surface, which we regard as one of the two rational elliptic surfaces arising in the stable degeneration limit of a K3 surface. It may also be thought of as the total space of a Seiberg-Witten curve (with the “ u ”-plane being the base) of an $\mathcal{N} = 2$ $SU(2)$ gauge theory or an E-string theory. In an affine patch of \mathbb{P}^1 with the coordinate z , the coefficient functions $f(z)$ and $g(z)$ are a 4th and a 6th order polynomial in z .⁵

As is well known, the modulus τ of the elliptic fiber of (1) is given by the implicit function:

$$J(\tau) = \frac{4f^3}{4f^3 + 27g^2}, \tag{2}$$

where J is the elliptic modular function. The denominator of the right hand side

$$\Delta \equiv 4f^3 + 27g^2 \tag{3}$$

is called the discriminant. Near its zero locus $z = z_i$, $\text{Im}\tau$ goes to ∞ (if one has chosen the “standard” fundamental region) for generic (that is, nonzero) f and g . Examining the behavior of $J(\tau)$ around ∞ , we find

$$\tau(z) = \frac{1}{2\pi i} \log(z - z_i) (\text{const.} + O(z - z_i)), \tag{4}$$

⁵ Although we introduce and define various notions in this simple setup, most of them can be generalized to a lower-dimensional F-theory compactification on a higher-dimensional elliptic Calabi-Yau, whose base \mathcal{W} is a \mathbb{P}^1 fibration over some base manifold \mathcal{B} , by simply taking y , x , f and g to be sections of $K_{\mathcal{W}}^{-3}$, $K_{\mathcal{W}}^{-2}$, $K_{\mathcal{W}}^{-4}$ and $K_{\mathcal{W}}^{-6}$, respectively, where $K_{\mathcal{W}}$ is the canonical class of \mathcal{W} . The equation (1) then describes a K3 fibered Calabi-Yau over \mathcal{B} . A configuration of the elliptic point planes, D-branes and various walls are then a “snapshot” of a \mathbb{P}^1 fiber over some point on \mathcal{B} with fixed coordinates.

which implies the existence of a D7-brane at each discriminant locus.⁶

On the other hand, since a locus of $f(z) = 0$ or $g(z) = 0$ alone does not mean $\Delta = 0$, it is not a D-brane. However, if the loci of $f(z) = 0$ and $g(z) = 0$ are present together with a D-brane, they play a significant role in generating a (p, q) -7-brane by acting $SL(2, \mathbb{Z})$ conjugate transformations on a D-brane or as components of an orientifold plane, as we show below. In this paper, we will collectively call the loci of $f(z) = 0$ and $g(z) = 0$ “*elliptic point planes*”.⁷

Elliptic point planes consist of two types, the loci of $f(z) = 0$ and $g(z) = 0$, which have different properties. In this paper, we call the locus of $f(z) = 0$ an $f=0$ *locus plane*, or an f -*plane* for short, and that of $g(z) = 0$ a $g=0$ *locus plane*, or a g -*plane* for short.⁸

At the location of an f -plane, the value of the J -function is

$$J(\tau) = \frac{4f^3}{4f^3 + 27g^2} = 0, \quad (5)$$

which corresponds to $\tau = e^{\frac{2\pi i}{3}}$. On the other hand, at the position of a g -plane,

$$J(\tau) = \frac{4f^3}{4f^3 + 27g^2} = 1, \quad (6)$$

so this implies $\tau = i$. In their neighborhoods, $J(\tau)$ is expanded as

$$J(\tau) = \frac{1}{3!} J'''(e^{\frac{2\pi i}{3}})(\tau - e^{\frac{2\pi i}{3}})^3 + O\left((\tau - e^{\frac{2\pi i}{3}})^4\right), \quad (7)$$

$$J(\tau) = 1 - \frac{12K\left(\frac{1}{\sqrt{2}}\right)^4}{\pi^2}(\tau - i)^2 + O((\tau - i)^3), \quad (8)$$

where $K(k)$ is the complete elliptic integral of the first kind

$$K(k) = \int_0^{\frac{\pi}{2}} \frac{d\theta}{\sqrt{1 - k^2 \sin^2 \theta}}. \quad (9)$$

Thus $\tau = e^{\frac{2\pi i}{3}}$ is a triple zero of $J(\tau)$ and $\tau = i$ is a double zero of $J(\tau) - 1$.

⁶ Thus, henceforth in this paper, we refer to a locus of the discriminant as (a locus of) a “D-brane”. As we will see, however, the monodromy around it is not always T (13) for a general choice of the reference point, due to the presence of the elliptic point planes.

⁷ In the standard fundamental region of the modular group of a two-torus, there are two elliptic points $\tau = e^{\frac{2\pi i}{3}}$ and i . They are fixed points of actions of some elliptic elements of $SL(2, \mathbb{Z})$, hence the name.

⁸ Despite the name “plane”, an elliptic point plane is no more a rigid object but a smooth submanifold when the elliptic fibration over \mathbb{P}^1 is further fibered over another manifold, just like a D-brane.

Suppose that $z = 0$ is a locus of $f = 0$. Since

$$J(\tau(z)) = \frac{4f(z)^3}{4f(z)^3 + 27g(z)^2}, \quad (10)$$

$J(\tau(z))$ is $O(z^3)$ at $z = 0$. So (7) shows that $\tau - e^{\frac{2\pi i}{3}}$ is $O(z)$ there, implying that the monodromy is trivial around the locus of f . Similarly, if $z = 0$ is a locus of $g = 0$, $J(\tau(z)) - 1$ is now $O(z^2)$. Comparing this with (8), we see that $\tau(z) - i$ is also $O(z)$, and hence there is no monodromy around the locus of $g = 0$, either.

However, this is not the end of the story. Figure 2 shows the various choices of fundamental regions of the modulus τ and the corresponding complex plane as its image mapped by the J -function. From this we can see that if one goes around $\tau = e^{\frac{2\pi i}{3}}$ once on the upper half plane, one goes through *three* different fundamental regions to get back to the original position. Likewise if one goes around $\tau = i$, one undergoes *two* different fundamental regions. Thus an f -plane is a complex codimension-one submanifold at which three different regions on the z -plane corresponding to different fundamental regions meet, while a g -plane is similarly the place where two different regions meet. The regions on the z -plane corresponding to different fundamental regions are bounded by real codimension-one domain walls which consist of the zero loci of the imaginary part of the J -function.

Furthermore, each region on the z -plane corresponding to a definite fundamental region is divided by a domain wall

$$\{\tau \mid \text{Im}J(\tau) = 0, \text{Re}J(\tau) > 1\} \quad (11)$$

(a dashed green line) into two regions $\text{Im}J(\tau) > 0$ and $\text{Im}J(\tau) < 0$.

On the other hand, a D-brane resides at a discriminant locus $\Delta = 0$, from which two domain walls $\{\tau \mid \text{Im}J(\tau) = 0, \text{Re}J(\tau) < 0\}$ (a green line) and $\{\tau \mid \text{Im}J(\tau) = 0, \text{Re}J(\tau) > 1\}$ (a dashed green line) extend out into the bulk z space (\mathbb{P}^1) (Fig.1).

Since the value of J is ∞ at a discriminant locus for generic (*i.e.* nonzero) values of f and g , D-branes can never, by definition, touch nor pass through (a non-end point of) the domain walls because $\text{Im}J(\tau)$ must vanish at the domain walls.

In this way, the z -space ($= \mathbb{P}^1$) is divided into several “*cell regions*”, which correspond to different fundamental regions in the preimage of the J -function, by the domain walls extended from the elliptic point planes ($=f$ -planes and g -planes) and D-branes (Fig.1). In

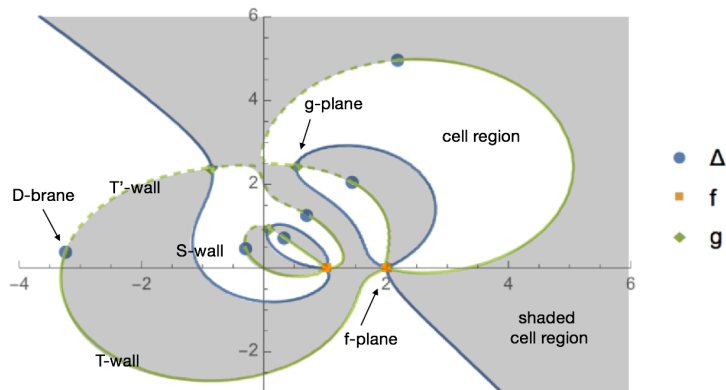


FIG. 1: An example configuration of D-branes, elliptic point planes and the cell regions bounded by the domain walls extended from them. D-branes are located at the loci of $\Delta = 0$, while elliptic point planes are at the loci of $f = 0$ and $g = 0$. In this example we can see two f -planes at $z = 1, 2$, three g -planes and six D-branes. (This figure is depicted for the Weierstrass equation (1) for f and g (44) with $\epsilon = 0.9$.)

particular, f -planes and g -planes extend the domain walls

$$\{\tau \mid \text{Im}J(\tau) = 0, 0 < \text{Re}J(\tau) < 1\} \quad (12)$$

(blue lines), and crossing through this wall implies that the type IIB coupling *locally gets S-dualized* (if starting from the standard choice of the fundamental region) (Fig.2). Then there is a difference in monodromies between when one goes around a D-brane within a single cell region bounded by some domain walls and when one first crosses through a domain wall, moves around a D-brane and then crosses back through the wall again to the original position; they are different by an $SL(2, \mathbb{Z})$ conjugation. This is what's happening in what has been called a “**B**-brane” or a “**C**-brane” in the discussions of string junctions. That is, while the monodromy matrix is necessarily

$$T = \begin{pmatrix} 1 & 1 \\ 0 & 1 \end{pmatrix} \quad (13)$$

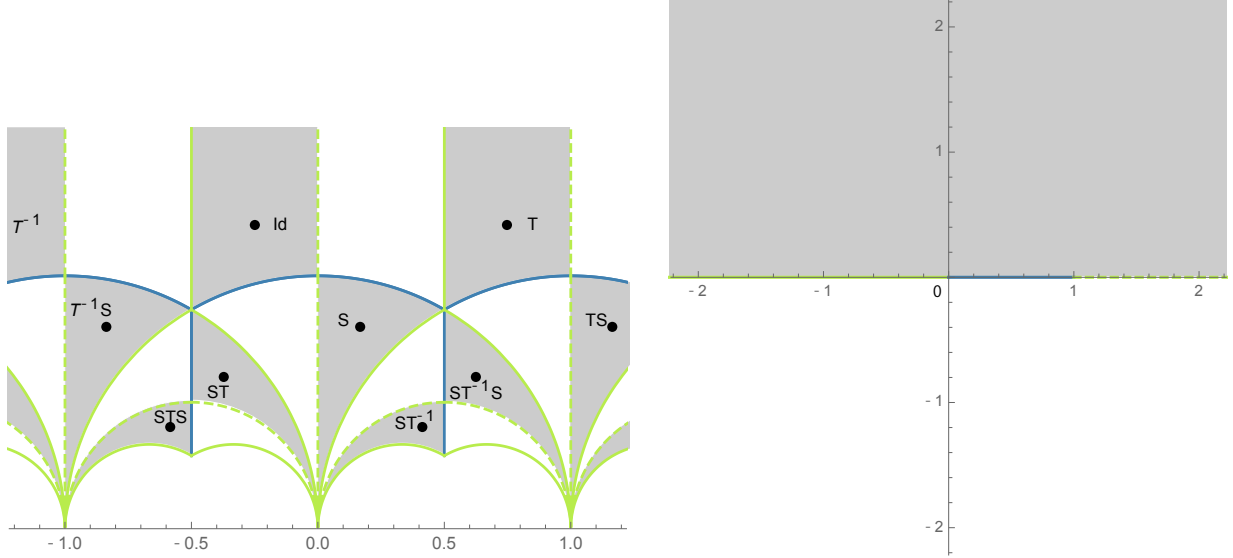


FIG. 2: Left: The upper half plane and various fundamental regions. The shaded regions are the regions in which the imaginary part of the image of the J -function $\text{Im}J(\tau)$ is positive. The symbol in each fundamental region (such as Id , T , S , ...) is the group element of $SL(2, \mathbb{Z})$ that maps the standard fundamental region to the fundamental region specified by the symbol. Right: The images of the J -function (= the whole complex plane). The green, blue and dashed green lines correspond to the respective boundary components of any one half of (the closure of) the fundamental regions.

as long as the reference point is chosen to be in the standard fundamental region, a non-trivial (non-D-brane) (p, q) -brane arises if the monodromy is measured by going back and forth between regions corresponding to different fundamental regions in the preimage upper-half plane.

We would like to emphasize here that such a local S transformation never takes place without these “elliptic point planes” (= f -planes and g -planes). If it were not for elliptic point planes but there are only D-branes, the domain walls extended from them are only the ones

$$\{\tau \mid \text{Im}J(\tau) = 0, \text{Re}J(\tau) < 0\} \quad (14)$$

(green lines) and

$$\{\tau \mid \text{Im}J(\tau) = 0, \text{Re}J(\tau) > 1\} \quad (15)$$

(dashed green lines). So crossing through these walls only leads to a T transformation which commutes with the original monodromies of D-branes.

In the discussion below, we refer to the domain wall (14) (a green lines) as T -wall and the one (15) (a dashed green line) as T' -wall, whereas we call the type of domain wall (12) (a blue line) S -wall.

To conclude this section we summarize the definitions of the new objects and notions introduced in this section as a mini-glossary.

Mini-glossary

f -plane A (complex) co-dimension-1 object corresponding to a zero locus of $f(z)$ in the Weierstrass form on the z -plane. Represented by a small square in the figures.

g -plane A (complex) co-dimension-1 object corresponding to a zero locus of $g(z)$ in the Weierstrass form on the z -plane. Represented by a small 45°-rotated square in the figures.

elliptic point plane The collective name for f -planes and g -planes.

T -wall A (real) co-dimension-1 object (domain wall) corresponding to a zero locus of $\text{Im}J$ with $\text{Re}J < 0$, extending from a D-brane and a f -plane. Represented by a green line.

T' -wall A (real) co-dimension-1 object (domain wall) corresponding to a zero locus of $\text{Im}J$ with $\text{Re}J > 1$, extending from a D-brane and a g -plane. Represented by a dashed green line.

S -wall A (real) co-dimension-1 object (domain wall) corresponding to a zero locus of $\text{Im}J$ with $0 < \text{Re}J < 1$, extending from a f -plane and a g -plane. Represented by a blue line.

cell region A closed region on the z -plane (\mathbb{P}^1 base of the elliptic fibration) bounded by the T -, T' - and S -walls. Each cell region corresponds to either half of the (closure of the) ⁹ fundamental region with $\text{Im}J > 0$ or $\text{Im}J < 0$ of the fiber modulus.

shaded cell region The cell region corresponding to the (closure of the) half fundamental region with $\text{Im}J > 0$ (Figure 1).

III. RELATION TO “DESSIN D’ENFANT” OF GROTHENDIECK

In fact, the construction in the previous section is nothing but drawing a “dessin d’enfant” of Grothendieck [60], known in mathematics, on the \mathbb{P}^1 base with a canonical triangulation.¹⁰

⁹ Below we abuse terminology and refer to a “fundamental region” as one modulo points on its boundary.
¹⁰ The contents of this section are triggered by a suggestion made by the anonymous referee of Phys. Rev. D.

A dessin d'enfant, meaning a drawing of a child, is a graph consisting of some black points, white points and lines connecting these points, drawn according to a special rule. To demonstrate the rule, let us consider, for example, a function [61]:

$$F(x) = -\frac{(x-1)^3(x-9)}{64x} = 1 - \frac{(x^2 - 6x - 3)^2}{64x}, \quad (16)$$

where $x \in \mathbb{P}^1$. F is a map from \mathbb{P}^1 to \mathbb{P}^1 . At almost everywhere on \mathbb{P}^1 , F is a homeomorphism, sending a small disk to another in a one-to-one way. However, F maps a small disk centered at $x = 1$ to one centered at $F = 0$ in a three-to-one way. Similarly, F is a two-to-one map from a small disk centered at $x = 3 \pm 2\sqrt{3}$ to one centered at $F = 1$. The points $x = 1, 3 \pm 2\sqrt{3}$ are said *critical points*, and the corresponding values of F are said *critical values*. If the map from the neighborhood around a critical point to another around the corresponding critical value is k -to-one, we say that the *ramification index* of the critical point is k .

Now the rule to draw the dessin associated with (16) is as follows: Place a black point at every preimage of 0, and a white point at every preimage of 1. Next draw lines at preimages of the line segment $[0, 1]$. The result is shown in FIG.3(a):

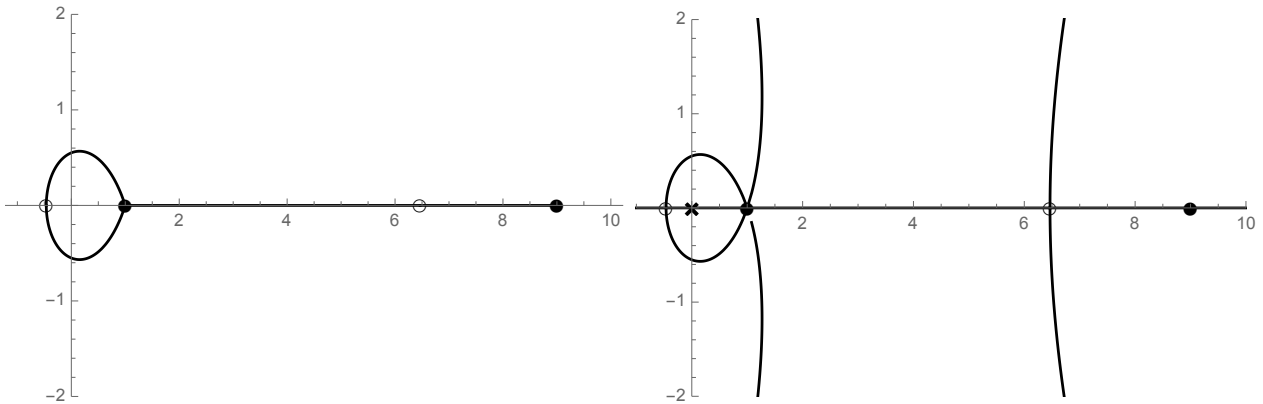


FIG. 3: (a)(left panel): The dessin for (16). (b)(right panel): The triangulated dessin. \times represents an ∞ point. The extra lines have been drawn at the preimages of the segment $[-\infty, 0]$ and $[1, \infty]$. The other ∞ point is not shown in this figure as it is infinitely far away.

The equation (16) induces a branched covering over \mathbb{P}^1 . Treating this graph as a combinatorial object, one can reproduce the information of the branched covering as follows: One first adds a point ∞ to each region of the dessin. One then connects each ∞ with lines to the black or white points as many times as they appear on the boundary of the region. This

yields a triangulation of the dessin. Assigning either the upper- or the lower-half plane to each triangle depending on the ordering of 0, 1, ∞ , and glueing these half planes together, one obtains a branched covering equivalent to the original one [61].

In the present case, the equation (10) defines a Belyi function, a holomorphic function whose critical values are only 0, 1 and ∞ and nothing else. The black and white points in the dessin shown in FIG.3(a) correspond to the f -planes and g -planes. The points ∞ added in the triangulation of the dessin are D-branes. The lines shown in FIG.3(a) are the S -walls, while the lines connecting the ∞ points and the black or white points drawn in the triangulation are the T - and T' -walls.

What is special about (10) is that it induces a local homeomorphism between the \mathbb{P}^1 base and the upper-half plane. Indeed, as we saw in the previous section, the correspondence is one-to-one everywhere, even in the vicinity of the elliptic orbits $\tau = e^{\frac{2\pi i}{3}}$ and i . This is so because the $J = 0$ ($f = 0$) points are always critical points with ramification index three, and the $J = 1$ ($g = 0$) points are always with ramification index two. In this paper, we treat the dessin not as just a combinatorial graph, but draw the ∞ points and the triangulating lines (the T - and T' -walls) also as preimages of the J -function, as shown in FIG.3(b). The special feature of (10) then allows us to use the (triangulated) dessin as a convenient tool to compute monodromies, as we see below.

IV. BASIC PROPERTIES OF ELLIPTIC POINT PLANES

A. Basic properties of f -planes

As we defined in the previous sections, there are two kinds of elliptic point planes: f -planes and g -planes. In this section we describe the basic properties of f -planes.

As the name indicates, f -planes are the loci where the function f vanishes. As we saw in the previous section, these are the places where the J -function vanishes and τ becomes $e^{\frac{2\pi i}{3}}$ (or its $SL(2, \mathbb{Z})$ equivalents).

As we saw in the previous section, the expansion of $J(\tau)$ near $\tau = e^{\frac{2\pi i}{3}}$ is given by (7). If there is an f -plane at $z = 0$, $f = 0$ there, yielding

$$f(z) = f_{41}z + f_{42}z^2 + \dots, \quad (17)$$

$$g(z) = g_{60} + g_{61}z + g_{62}z^2 + \dots, \quad (18)$$

where f_{4i} , g_{6j} are constants with indices running over $i = 1, \dots, 8$ and $j = 1, \dots, 12$ for a K3 surface and $i = 1, \dots, 4$ and $j = 1, \dots, 6$ for a rational elliptic surface. Since

$$\frac{4f^3}{4f^3 + 27g^2} = \frac{4f_{41}^3}{27g_{60}^2} z^3 (1 + O(z)), \quad (19)$$

$\tau(z)$ asymptotically approaches

$$\tau(z) = e^{\frac{2\pi i}{3}} + \frac{2f_{41}}{(9g_{60}^2 J'''(e^{\frac{2\pi i}{3}}))^{\frac{1}{3}}} z \quad (20)$$

as $z \rightarrow 0$. Therefore, τ is regular near $z = 0$, and hence an f -plane does not carry D-brane charges.

Parameterize a small circle around $z = 0$ by $z = \epsilon e^{i\theta}$ ($\epsilon > 0$), then if one goes around along it once, so does τ once around $e^{\frac{2\pi i}{3}}$ along a small circle with a radius $\epsilon \left| \frac{2f_{41}}{(9g_{60}^2 J'''(e^{\frac{2\pi i}{3}}))^{\frac{1}{3}}} \right|$. Thus, although the monodromy around an f -plane is trivial, one passes through the boundary of the half-fundamental region *six* times on the upper-half plane as one goes once around an f -plane. Since the neighborhoods of $z = 0$ and $\tau = e^{\frac{2\pi i}{3}}$ are homeomorphic, the neighborhood of $z = 0$ around an f -plane is also divided into six cell regions corresponding to different half-fundamental regions. The six domain walls separating these cell regions consist of three S -walls (blue) with $(0 < \text{Re}J(\tau) < 1)$ and three T -walls (green) ($\text{Re}J(\tau) < 0$), which are extended alternately from the f -plane, forming a locally \mathbb{Z}_3 -symmetric configuration.

On the upper-half plane, if one starts from the standard fundamental region and passes through preimages (of the J -function) of a T -wall (green) and an S -wall (blue) to go to the $SL(2, \mathbb{Z})$ equivalent point, then the $SL(2, \mathbb{Z})$ transformation mapping the original point to the final point is $T^{-1}S$. Further, if one crosses through preimages of a T -wall (green) and an S -wall (blue) again, the transformation to the final $SL(2, \mathbb{Z})$ equivalent point is $(T^{-1}S)^2 = -ST \sim ST$ (as $PSL(2, \mathbb{Z})$).

Since

$$(T^{-1}S)^3 = 1, \quad (21)$$

$T^{-1}S$ generates a \mathbb{Z}_3 group, which is the isotropy group of the elliptic point $\tau = e^{\frac{2\pi i}{3}}$. It is easy to show that this $T^{-1}S$ transformation acts on the neighborhood of this point as a $\frac{2\pi i}{3}$ rotation. Therefore, the configuration of τ near an f -plane is locally invariant under the simultaneous actions of the spacial \mathbb{Z}_3 rotation and the \mathbb{Z}_3 $SL(2, \mathbb{Z})$ transformation. The metric near an f -plane is locally \mathbb{Z}_3 invariant.

B. Basic properties of g -planes

Likewise, the expansion of $J(\tau)$ around $\tau = i$ is given by (8). Let a g -plane be at $z = 0$ this time. $f(z)$ and $g(z)$ are expanded as

$$f(z) = f_{40} + f_{41}z + f_{42}z^2 + \dots, \quad (22)$$

$$g(z) = g_{61}z + g_{62}z^2 + \dots. \quad (23)$$

Since

$$\frac{4f^3}{4f^3 + 27g^2} = 1 - \frac{27g_{61}^2}{4f_{40}^3}z^2(1 + O(z)), \quad (24)$$

$\tau(z)$ approaches

$$\tau(z) = i + \frac{3i\pi^{\frac{1}{2}}g_{61}}{4K(\frac{1}{\sqrt{2}})^2f_{40}^{\frac{3}{2}}}z \quad (25)$$

as $z \rightarrow 0$. Thus τ is again regular near a g -plane, therefore a g -plane does not have D-brane charges, either. The monodromy around a g -plane is also trivial, although if one goes around it, one will be passing through the S -walls (blue lines) and the T' -walls (dashed green lines) alternately, twice for each.

Suppose that on the upper-half plane one starts from an arbitrarily given point near $\tau = i$ in the standard fundamental region with $\text{Re}\tau < 0$ and goes through the preimages of an S -wall and a T' -wall to reach the $SL(2, \mathbb{Z})$ -equivalent point. This move can be achieved by the $SL(2, \mathbb{Z})$ S transformation. This S transformation acts on the neighborhood of $\tau = i$ as a \mathbb{Z}_2 rotation. The metric near a g -plane is also $SL(2, \mathbb{Z})$ invariant. Thus the vicinity of a g -plane is invariant under the \mathbb{Z}_2 rotation associated with the S transformation.

V. SIMPLE METHOD TO COMPUTE THE MONODROMY USING THE DESSIN

Drawing the contours of the walls and the positions of the D-branes and elliptic point planes, we can have a figure of the complex plane divided into several cell regions such as FIG.1, which we call a *dessin*.¹¹ For a given Weierstrass equation, the dessin provides us

¹¹ This corresponds to a *triangulated* dessin in the sense of Grothendieck.

with a very simple method to compute the monodromy matrices along an arbitrary path around branes on the complex plane (= an affine patch of the \mathbb{P}^1 or the “ u -plane” of a Seiberg-Witten curve).

A. The method

To illustrate the method, let us consider the Seiberg-Witten curve of $\mathcal{N} = 2$ pure ($N_f = 0$) $SU(2)$ supersymmetric gauge theory [62]. The equation is

$$y^2 = x^3 - ux^2 + x. \quad (26)$$

Taking u as the coordinate z , we obtain a Weierstrass equation with

$$f(u) = -\frac{1}{3}u^2 + 1, \quad g(u) = -\frac{2}{27}u^3 + \frac{1}{3}u, \quad (27)$$

whose dessin is shown in the upper panel of Figure 4. Let us compute the monodromy around each discriminant locus. Choosing a starting point near the left locus (shown as a cross), the left path crosses the walls as

$$\rightarrow \mathbf{G} \rightarrow \mathbf{B} \rightarrow \mathbf{G} \rightarrow \mathbf{dG} \rightarrow, \quad (28)$$

where \mathbf{G} denotes the T -wall, \mathbf{B} the S -wall and \mathbf{dG} the T' -wall.¹² The monodromy matrices for various patterns of crossings are

$$\begin{aligned} \rightarrow \mathbf{dG} \rightarrow \mathbf{G} \rightarrow &= T, \\ \rightarrow \mathbf{G} \rightarrow \mathbf{dG} \rightarrow &= T^{-1}, \\ \rightarrow \mathbf{dG} \rightarrow \mathbf{B} \rightarrow &= \rightarrow \mathbf{B} \rightarrow \mathbf{dG} \rightarrow = S, \\ \rightarrow \mathbf{B} \rightarrow \mathbf{G} \rightarrow &= ST, \\ \rightarrow \mathbf{G} \rightarrow \mathbf{B} \rightarrow &= T^{-1}S, \end{aligned} \quad (29)$$

where the first wall of each row is the crossing from a shaded cell region ($\text{Im}J > 0$) to an unshaded one ($\text{Im}J < 0$), and the second is from an unshaded to a shaded one.¹³ The

¹² \mathbf{G} , \mathbf{B} and \mathbf{dG} are respectively the first letters of Green, Blue and dashed Green. We have avoided using T , S or T' here as the monodromy matrices for the crossing do not coincide with the names of the walls.

¹³ Therefore, these rules only apply when one computes a monodromy for a path that starts from and ends in a *shaded cell region* ($\text{Im}J > 0$). The rules for computing a monodromy for a path from an *unshaded*

monodromy matrices are defined as

$$T = \begin{pmatrix} 1 & 1 \\ 0 & 1 \end{pmatrix}, \quad S = \begin{pmatrix} 0 & -1 \\ 1 & 0 \end{pmatrix} \quad (31)$$

as usual, where we say that the monodromy matrix is $\begin{pmatrix} a & b \\ c & d \end{pmatrix}$ if the modulus τ is changed to

$$\tau' = M \circ \tau \equiv \frac{a\tau + b}{c\tau + d}. \quad (32)$$

They are defined only in $PSL(2, \mathbb{Z})$, *i.e.* up to a multiplication of -1 .

By using the rule (29), we can immediately find the monodromy matrix for the path (28) as

$$\begin{aligned} T^{-1}S \cdot T^{-1} &= T^{-1}ST^{-1} \\ &\sim STS, \end{aligned} \quad (33)$$

where \sim denotes the equality in $PSL(2, \mathbb{Z})$.

Similarly, the crossed walls for the right path are

$$\rightarrow \mathbf{G} \rightarrow \mathbf{dG} \rightarrow \mathbf{G} \rightarrow \mathbf{dG} \rightarrow \mathbf{G} \rightarrow \mathbf{dG} \rightarrow \mathbf{B} \rightarrow \mathbf{G} \rightarrow . \quad (34)$$

Using rule (29) again, we find that the monodromy is

$$T^{-1} \cdot T^{-1} \cdot T^{-1} \cdot ST = T^{-3}ST. \quad (35)$$

A confusing but important point of the rule is that, in the first example, the monodromy matrix T^{-1} which corresponds to the crossings $\rightarrow \mathbf{G} \rightarrow \mathbf{dG} \rightarrow$ taking place *after* the

cell region ($\text{Im}J < 0$) to another are similar but different:

$$\begin{aligned} \rightarrow \mathbf{dG} \rightarrow \mathbf{G} \rightarrow &= T^{-1}, \\ \rightarrow \mathbf{G} \rightarrow \mathbf{dG} \rightarrow &= T, \\ \rightarrow \mathbf{dG} \rightarrow \mathbf{B} \rightarrow &= \rightarrow \mathbf{B} \rightarrow \mathbf{dG} \rightarrow = S, \\ \rightarrow \mathbf{B} \rightarrow \mathbf{G} \rightarrow &= ST^{-1}, \\ \rightarrow \mathbf{G} \rightarrow \mathbf{B} \rightarrow &= TS. \end{aligned} \quad (30)$$

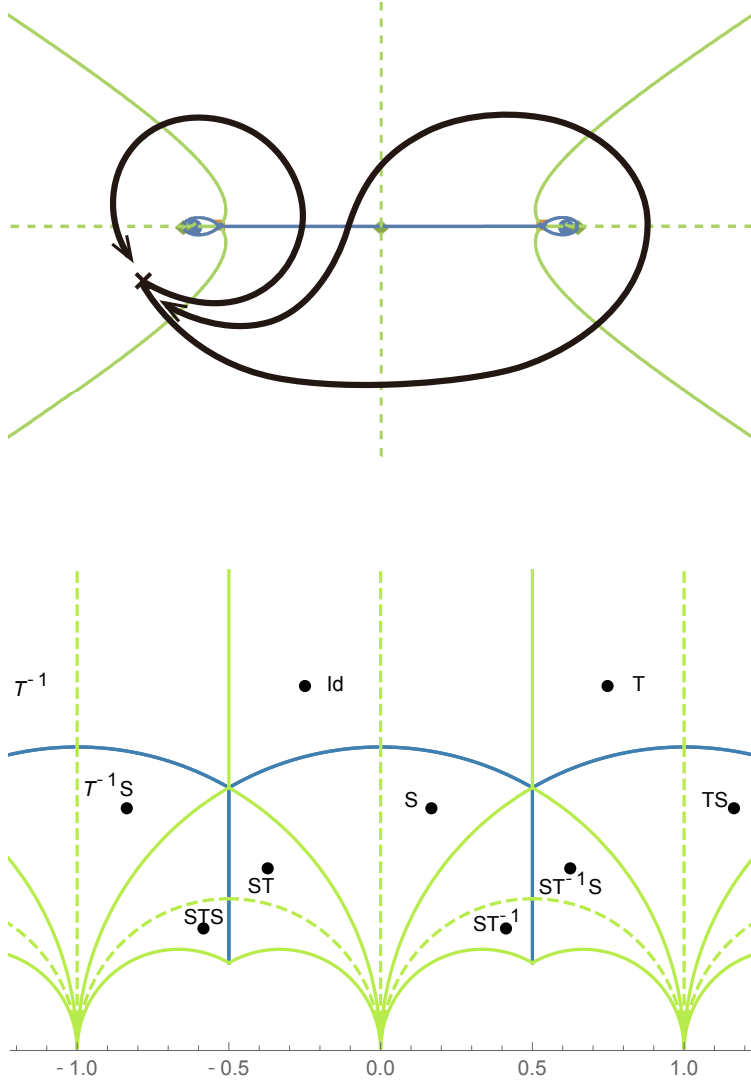


FIG. 4: The upper panel: The dessin of $N_f = 0$ SW curve ($f(u) = -\frac{1}{3}u^2 + 1$, $g(u) = -\frac{2}{27}u^3 + \frac{1}{3}u$). The lower panel: The crossed walls and the corresponding monodromies.

crossings $\rightarrow \mathbf{G} \rightarrow \mathbf{B} \rightarrow$ is multiplied to $T^{-1}S$ from the *right*. This will be confusing because if $M = \begin{pmatrix} a & b \\ c & d \end{pmatrix}$, $M' = \begin{pmatrix} a' & b' \\ c' & d' \end{pmatrix}$ and $\tau' = M \circ \tau$, $\tau'' = M' \circ \tau'$, then the monodromy matrix $M'' = \begin{pmatrix} a'' & b'' \\ c'' & d'' \end{pmatrix}$ representing $\tau \mapsto \tau'' = M'' \circ \tau$ is given by

$$M'' = M'M, \tag{36}$$

in which M' is multiplied from the *left*.

More generally, the following statement holds: Let γ be a path specified by the series of the walls

$$\gamma : \rightarrow \mathbf{W}_1 \rightarrow \mathbf{W}_2 \rightarrow \cdots \rightarrow \mathbf{W}_k \rightarrow, \quad (37)$$

where \mathbf{W}_i ($i = 1, \dots, k$) are either of \mathbf{G} , \mathbf{B} or \mathbf{dG} , and let M_γ denote the associated monodromy matrix of γ . k is an even positive integer. (If it is odd, a shaded cell region is mapped to an unshaded cell region or vice versa, and the transformation cannot be an $SL(2, \mathbb{Z})$ transformation). Let γ_1, γ_2 be paths specified by the series of the walls crossed by them

$$\begin{aligned} \gamma_1 &: \rightarrow \mathbf{W}_1^{(1)} \rightarrow \mathbf{W}_2^{(1)} \rightarrow \cdots \rightarrow \mathbf{W}_{k_1}^{(1)} \rightarrow, \\ \gamma_2 &: \rightarrow \mathbf{W}_1^{(2)} \rightarrow \mathbf{W}_2^{(2)} \rightarrow \cdots \rightarrow \mathbf{W}_{k_2}^{(2)} \rightarrow, \end{aligned} \quad (38)$$

and let $\gamma_1 \bowtie \gamma_2$ be the jointed path

$$\gamma_1 \bowtie \gamma_2 : \rightarrow \mathbf{W}_1^{(1)} \rightarrow \cdots \rightarrow \mathbf{W}_{k_1}^{(1)} \rightarrow \mathbf{W}_1^{(2)} \rightarrow \cdots \rightarrow \mathbf{W}_{k_2}^{(2)} \rightarrow, \quad (39)$$

where we use the new symbol \bowtie to denote the operation of jointing two paths.¹⁴ Then

Proposition.

$$M_{\gamma_1 \bowtie \gamma_2} = M_{\gamma_1} M_{\gamma_2}. \quad (40)$$

Remark. As we noted above, the monodromy matrix corresponding to a later crossing comes to the *right*, unlike (36) in which the matrix for the later transformation is multiplied from the *left*.

Proof. By induction with respect to the total number of crossed walls, it is enough to show the statement for the cases when γ_2 is any of the crossing patterns (29). Suppose that γ_1 starts from a cell region C_0 and ends in another C_1 , and that γ_2 goes from the cell region C_1 to another C_2 , where γ_2 is taken to be any of the crossing patterns (29), say, $\gamma_2 \Rightarrow \mathbf{dG} \rightarrow \mathbf{G} \rightarrow$ and $M_{\gamma_2} = T$. Let P_{γ_i} ($i = 1, 2$) be the associated maps which send points in the cell region C_{i-1} to those in the cell region C_i , respectively, such that

¹⁴ We will not use the usual symbol for the addition “+” since this operation is noncommutative.

the torus modulus over the point is $SL(2, \mathbb{Z})$ equivalent. We say two points on \mathbb{P}^1 are $SL(2, \mathbb{Z})$ equivalent if the torus fiber moduli over them are $SL(2, \mathbb{Z})$ equivalent. Using this terminology, we can say that P_{γ_i} ($i = 1, 2$) are the maps which send the points in C_{i-1} to their $SL(2, \mathbb{Z})$ equivalent points in C_i , respectively. Since $\tau(z)$ is holomorphic in z and $J(\tau)$ is holomorphic in τ , the domain of the map P_{γ_1} is not necessarily restricted to only C_0 but can be extended to outside C_0 as far as it is in a small neighborhood of z_0 .

Let z_0 be a point in C_0 , and let $z_1 = P_{\gamma_1}(z_0) \in C_1$, $z_2 = P_{\gamma_2}(z_1) \in C_2$. If we denote τ_i ($i = 0, 1, 2$) be the modulus of the torus fiber over z_i ($i = 0, 1, 2$), they satisfy

$$J(\tau_i) = \frac{4f(z_i)^3}{4f(z_i)^3 + 27g(z_i)^2}, \quad (41)$$

where τ_1 and τ_2 are the values analytically continued from τ_0 along the paths γ_1 , and then γ_2 . Taking τ_0 in the *standard* fundamental region, the transformation from τ_0 to τ_1 is given by $\tau_1 = M_{\gamma_1} \circ \tau_0$, but consecutive transformation from τ_1 to τ_2 is *not* $M_{\gamma_2} \circ \tau_1$, as τ_1 does not belong to the standard fundamental region in general. Rather, since P_{γ_1} is locally an isomorphism between a neighborhood around z_0 and that around z_1 , the final point z_2 can be written as the P_{γ_1} image of z'_1 , where z'_1 is the $SL(2, \mathbb{Z})$ equivalent point in the cell region *reached along the path γ_2 first* from z_0 , if z_2 is close enough to z_1 (Figure 5). If, on the other hand, z_2 is not close to z_1 , we can continuously deform the complex structure of the elliptic fibration so that z_2 may come close to z_1 . Since this is a continuous deformation, the monodromy transformation matrix does not change, as the entries of the matrix take discrete values. Thus we may assume that z_2 is close to z_1 .

Since τ_0 is taken in the standard fundamental region, τ'_1 , the modulus of the torus fiber over z'_1 , is given by

$$\tau'_1 = M_{\gamma_2} \circ \tau_0. \quad (42)$$

Therefore, since $\tau_2 = M_{\gamma_1} \circ \tau'_1$, we find

$$\begin{aligned} \tau_2 &= M_{\gamma_1} \circ M_{\gamma_2} \circ \tau_0 \\ &= (M_{\gamma_1} M_{\gamma_2}) \circ \tau_0, \end{aligned} \quad (43)$$

which is what the proposition claims.

In deriving (43), we did not use the fact that γ_2 was assumed to be a particular pattern among (29), but the relation (43) likewise holds for other patterns. This completes the proof

of the proposition.¹⁵

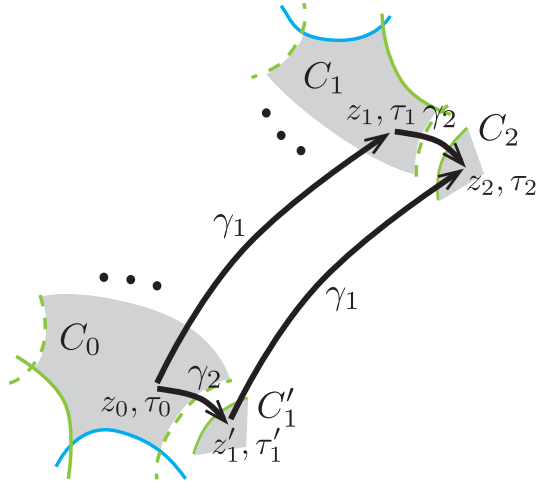


FIG. 5: Taking τ_0 in the *standard* fundamental region, the transformation from τ_0 to τ_1 is given by $\tau_1 = M_{\gamma_1} \circ \tau_0$, but consecutive transformation from τ_1 to τ_2 is *not* $M_{\gamma_2} \circ \tau_1$, as τ_1 does not belong to the standard fundamental region in general. Rather, we have $\tau_2 = M_{\gamma_1} \circ \tau'_1$ with $\tau'_1 = M_{\gamma_2} \circ \tau_0$ as P_{γ_1} induces an isomorphism.

B. Example: Monodromies of $N_f = 4$ $SU(2)$ Seiberg-Witten curves

The proposition (40) together with the rule (29) provides us with a very convenient method to compute the monodromy for an arbitrary Weierstrass model along an arbitrary path.

Figure 6 is a dessin of $N_f = 4$ $SU(2)$ Seiberg-Witten curve with some mass parameters.

¹⁵ In this proof, γ_2 is taken to be a path to the next adjacent cell region, whereas γ_1 is assume to be some long path leading to a faraway cell region. If γ_1 is also a path to another next adjacent cell region, it can be explicitly checked that the proposition holds in this case as well.

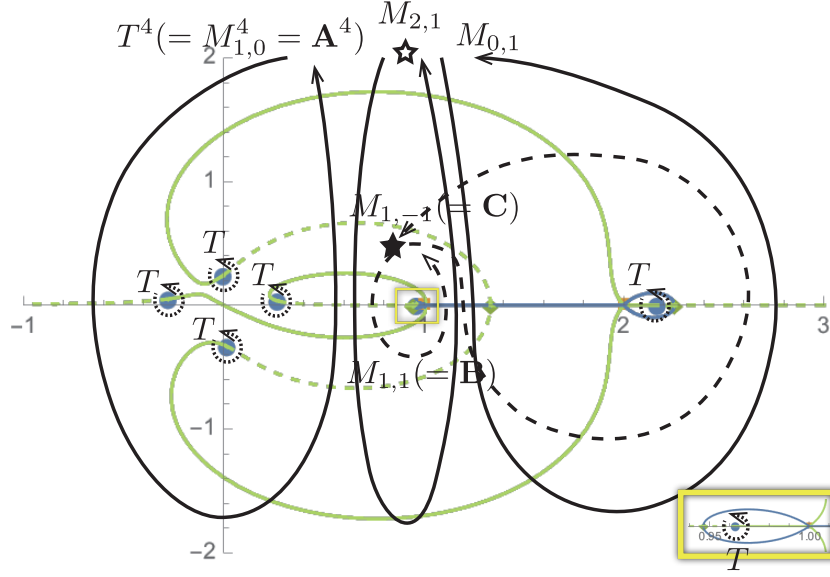


FIG. 6: Monodromies of $N_f = 4$ $SU(2)$ Seiberg-Witten curve. It shows how the monodromies around the two D-branes on the right (located at $z \approx 1$ and ≈ 2) change depending on the choice of the reference point. If it is taken far enough (as marked as a white star), the monodromies along the black contours read $M_{2,1}$ and $M_{0,1}$. If the reference point is taken closer (as marked as a black star), then the monodromies along the dashed black contours are $M_{1,1}(= \mathbf{B})$ and $M_{1,-1}(= \mathbf{C})$. If, on the other hand, the reference point is taken to be very close to the D-branes inside the cell regions surrounded by the S -walls, then the monodromies along the dotted contours are both T .

The Weierstrass equation is (1) where

$$\begin{aligned}
 f &= (z - 1)(z - 2), \\
 g &= \epsilon(z - i)(z - 2i)(z - 3i) \\
 &\quad + (1 - \epsilon) \left(-\frac{5}{16}i\sqrt{\frac{3}{2}}z^3 + \frac{17iz^2}{4\sqrt{6}} - i\sqrt{6}z + \frac{4}{3}i\sqrt{\frac{2}{3}} \right)
 \end{aligned} \tag{44}$$

with $\epsilon = 3 \times 10^{-7}$. This choice of g interpolates between the configuration in which all the g -locus planes are located on the imaginary axis at equal intervals ($\epsilon = 1$) and the one in which four of the six D-branes collide together at $z = 0$ to form a I_4 singular fiber ($\epsilon = 0$), with the f -planes fixed at $z = 1, 2$. The figure is the configuration very close to the latter limit.

As is well known, the one-parameter (“ u ”) family of tori describe the moduli space of the gauge theory and can be compactified into a rational elliptic surface by taking the variables and coefficient functions to be sections of appropriate line bundles, where the u parameter becomes the affine coordinate z of the base \mathbb{P}^1 . Note, however, that the dessin can be drawn on this affine patch independently of the choices of the bundles; it only affects how many D-branes are at the infinity of \mathbb{P}^1 .

This figure shows how the monodromies around the two D-branes on the right (located at $z \approx 1$ and ≈ 2) change depending on the choice of the reference point. If it is taken far enough (as marked as a white star), the monodromies along the black contours read $M_{2,1}$ and $M_{0,1}$. This means that, as we show later, a $(2, 1)$ and a $(0, 1)$ string become light near the respective D-branes, showing that the locations of the D-branes are the $(2, 1)$ dyon and the monopole point on the moduli space of the gauge theory, which is well known.

If the reference point is taken closer (as marked as a black star), then the monodromies along the dashed black contours are $M_{1,1}(= \mathbf{B})$ and $M_{1,-1}(= \mathbf{C})$, which agrees with the **ABC** brane description of the I_0^* Kodaira singular fiber.

Finally, if the reference point is taken to be very close to the D-branes inside the cell regions surrounded by the S -walls, then the monodromies along the dotted contours are both T , showing that these branes look ordinary D-branes if they are observed from very close to them.

C. (p, q) -brane as an effective description

Of course, it is well known that the monodromy changes depending the choice of the reference point. A monodromy matrix measured from some reference point gets $SL(2, \mathbb{Z})$ conjugated if it is measured from another point. What is new here that, by drawing a dessin, we can precisely see how and from where the monodromy matrix changes and gets conjugated as we vary the position of the reference point.

For instance, we can see from Figure 6 that the monodromies around the two D-branes on the right are either $M_{2,1}$, $M_{0,1}$ or $M_{1,1}(= \mathbf{B})$, $M_{1,-1}(= \mathbf{C})$ for most choices of the reference point on the $z(\equiv u)$ -plane, and they are recognized as ordinary ($M_{1,0} = \mathbf{A}$) D-branes only when they are viewed from the points in the tiny regions surrounded by the S -walls. Thus we see that the effective description of the two branes as $(1, 1)(= \mathbf{B})$ - and $(1, -1)(= \mathbf{C})$ -

branes are good at the energy scale lower than the scale of the size of the small cell regions surrounded by the S -walls.

However, one can also set the mass parameters of the same gauge theory so that the dessin of the Seiberg-Witten curve looks as shown in Figure 1. In this case, the S -walls spread into wide areas of the \mathbb{P}^1 . There is not much difference among the six D-branes, and there is no obvious reason to distinguish particular two as **B** or **C** from the other four D-branes.

Remark. We have seen that a cluster of a D-brane and two elliptic point planes, in which the former is surrounded by the S -walls extended from the latter, may be effectively identified as a **B**- or a **C**-brane, if viewed from a distance of the size of the cluster. Thus one might think that an “exact” (p, q) -brane (whose monodromy is $M_{p,q}$ along arbitrary small loop) can be obtained by taking the f - and g -planes on top of each other so that the size of the cell region the S -walls surround becomes zero. This is not the case, however, since if the f - and g -planes collide, the order of the discriminant becomes two, implying that another D-brane also automatically comes on top of the D-brane, f -plane and g -plane. Since it contains two D-branes, it cannot be identified as a *single* (p, q) -brane in the **ABC**-brane description.

VI. CONCLUSIONS

The coexistence of D-branes and non-pure-D-7-branes is an essential feature of F-theory, as it enables us to achieve exceptional group gauge symmetries or matter in spinor representations by allowing string junctions to appear as extra objects ending on more than two different types of 7-branes, in addition to the open strings which can only connect two ordinary D-branes. These 7-branes are conventionally described algebraically in terms of **ABC** 7-branes. In this paper, noticing that all the discriminant loci are on equal footing and there is no a priori reason to distinguish one from the others, we have considered new complex co-dimension one objects consisting of the zero loci of the coefficient functions f and g of the Weierstrass equation, which we referred to as an “ f -plane” and a “ g -plane”, collectively as “elliptic point planes”. They are two kinds of critical points of a “dessin d’enfant” known in mathematics.

Although they do not carry D-brane charges, they play an essential role in achieving an

exceptional gauge symmetry and/or a spinor representation by altering the monodromies around the branes. More precisely, if there are some elliptic point planes, the z -plane is divided into several cell regions, each of which corresponds to a (half of a) fundamental region in the preimage of the J -function. A cell region is bounded by several domain walls extending from these elliptic point planes and D-branes, on which the imaginary part of the J -function vanishes. In particular, the elliptic point planes extend a special kind of domain walls, which we call “ S -walls”, crossing through which implies that the type IIB complex string coupling is S -dualized. Consequently, on the z -plane coexist a theory in the perturbative regime and its nonperturbative S -dual simultaneously. The monodromy around several 7-branes is thus not just a product of monodromy around each 7-brane any more, but they get $SL(2, \mathbb{Z})$ conjugated due to the difference of the corresponding fundamental regions the base points belong to.

In this sense one may say that the nonperturbative properties of F-theory — the realizations of exceptional group symmetry, matter in spinor representations, etc. — are the consequence of the coexisting “locally S -dualized regions” bounded by the S -walls extended from the elliptic point planes. In the orientifold limit [63], the D-branes and the elliptic point planes gather to form a I_0^* singular fiber, so that the S -walls extended from the elliptic point planes are contracted with each other and confined, so the S -walls are not seen from even a short distance.

We hope this new way of presenting the non-localness among 7-branes will be useful for understanding of the structure of higher-codimension singularities with higher-rank enhancement such as discussed in [2, 3, 11, 64–67].

Acknowledgments

We wish to thank the referee of Phys. Rev. D for suggesting the improvement of the manuscript by considering the mathematical concept of dessin d’enfant. We also thank Y. Kimura and T. Tani for valuable discussions. The work of S. M. is supported by Grant-in-Aid for Scientific Research (C) #16K05337 from The Ministry of Education, Culture, Sports, Science and Technology of Japan.

Appendix

TABLE I: The Kodaira classification. $\text{ord}(f)$, $\text{ord}(g)$ and $\text{ord}(\Delta)$ denote the orders of zeros of f , g and the discriminant Δ of the Weierstrass equation.

Fiber type	$\text{ord}(f)$	$\text{ord}(g)$	$\text{ord}(\Delta)$	Singularity type	7-brane configuration	Brane type
I_n	0	0	n	A_{n-1}	\mathbf{A}^n	A_{n-1}
II	≥ 1	1	2	A_0	\mathbf{CA}	H_0
III	1	≥ 2	3	A_1	\mathbf{CA}^2	H_1
IV	≥ 2	2	4	A_2	\mathbf{CA}^3	H_2
I_n^*	≥ 2	3	$6+n$	D_{n+4}	$\mathbf{A}^{n+4}\mathbf{BC}$	D_{n+4}
I_n^*	2	≥ 3	$6+n$	D_{n+4}	$\mathbf{A}^{n+4}\mathbf{BC}$	D_{n+4}
II^*	≥ 4	5	10	E_8	$\mathbf{A}^7\mathbf{BC}^2$	E_8
III^*	3	≥ 5	9	E_7	$\mathbf{A}^6\mathbf{BC}^2$	E_7
IV^*	≥ 3	4	8	E_6	$\mathbf{A}^5\mathbf{BC}^2$	E_6

-
- [1] C. Vafa, Nucl. Phys. B **469** (1996) 403 [hep-th/9602022].
- [2] D. R. Morrison and C. Vafa, Nucl. Phys. B **473** (1996) 74 [hep-th/9602114].
- [3] D. R. Morrison and C. Vafa, Nucl. Phys. B **476** (1996) 437 [hep-th/9603161].
- [4] E. Witten, Nucl. Phys. B **471** (1996) 135 [hep-th/9602070].
- [5] R. Blumenhagen, B. Kors, D. Lust and T. Ott, Nucl. Phys. B **616** (2001) 3 [hep-th/0107138].
- [6] R. Blumenhagen, M. Cvetič, D. Lust, R. Richter and T. Weigand, Phys. Rev. Lett. **100** (2008) 061602 [arXiv:0707.1871 [hep-th]].
- [7] R. Donagi and M. Wijnholt, Adv. Theor. Math. Phys. **15**, 1237 (2011) [arXiv:0802.2969 [hep-th]].
- [8] C. Beasley, J. J. Heckman and C. Vafa, JHEP **0901**, 058 (2009) [arXiv:0802.3391 [hep-th]].
- [9] C. Beasley, J. J. Heckman and C. Vafa, JHEP **0901**, 059 (2009) [arXiv:0806.0102 [hep-th]].
- [10] R. Donagi and M. Wijnholt, Adv. Theor. Math. Phys. **15**, 1523 (2011) [arXiv:0808.2223 [hep-th]].

- [11] H. Hayashi, T. Kawano, R. Tatar and T. Watari, Nucl. Phys. B **823** (2009) 47 [arXiv:0901.4941 [hep-th]].
- [12] R. Donagi and M. Wijnholt, Commun. Math. Phys. **326** (2014) 287 [arXiv:0904.1218 [hep-th]].
- [13] J. J. Heckman, J. Marsano, N. Saulina, S. Schafer-Nameki and C. Vafa, arXiv:0808.1286 [hep-th].
- [14] J. Marsano, N. Saulina and S. Schafer-Nameki, Phys. Rev. D **80** (2009) 046006 [arXiv:0808.1571 [hep-th]].
- [15] J. J. Heckman and C. Vafa, JHEP **0909** (2009) 079 [arXiv:0809.1098 [hep-th]].
- [16] A. Font and L. E. Ibanez, JHEP **0902** (2009) 016 [arXiv:0811.2157 [hep-th]].
- [17] R. Friedman, J. Morgan and E. Witten, Commun. Math. Phys. **187** (1997) 679 [hep-th/9701162].
- [18] H. Hayashi, R. Tatar, Y. Toda, T. Watari and M. Yamazaki, Nucl. Phys. B **806** (2009) 224 [arXiv:0805.1057 [hep-th]].
- [19] B. Andreas and G. Curio, J. Geom. Phys. **60** (2010) 1089 doi:10.1016/j.geomphys.2010.03.008 [arXiv:0902.4143 [hep-th]].
- [20] J. Marsano, N. Saulina and S. Schafer-Nameki, JHEP **0908** (2009) 030 [arXiv:0904.3932 [hep-th]].
- [21] A. Collinucci, JHEP **1004** (2010) 076 [arXiv:0906.0003 [hep-th]].
- [22] R. Blumenhagen, T. W. Grimm, B. Jurke and T. Weigand, JHEP **0909** (2009) 053 [arXiv:0906.0013 [hep-th]].
- [23] J. Marsano, N. Saulina and S. Schafer-Nameki, JHEP **0908** (2009) 046 [arXiv:0906.4672 [hep-th]].
- [24] R. Blumenhagen, T. W. Grimm, B. Jurke and T. Weigand, Nucl. Phys. B **829** (2010) 325 [arXiv:0908.1784 [hep-th]].
- [25] J. Marsano, N. Saulina and S. Schafer-Nameki, JHEP **1004** (2010) 095 [arXiv:0912.0272 [hep-th]].
- [26] T. W. Grimm, S. Krause and T. Weigand, JHEP **1007** (2010) 037 [arXiv:0912.3524 [hep-th]].
- [27] M. Cvetič, I. Garcia-Etxebarria and J. Halverson, JHEP **1101** (2011) 073 [arXiv:1003.5337 [hep-th]].
- [28] C. M. Chen, J. Knapp, M. Kreuzer and C. Mayrhofer, JHEP **1010** (2010) 057 [arXiv:1005.5735 [hep-th]].

- [29] C. M. Chen and Y. C. Chung, JHEP **1103** (2011) 049 [arXiv:1005.5728 [hep-th]].
- [30] T. W. Grimm and T. Weigand, Phys. Rev. D **82** (2010) 086009 [arXiv:1006.0226 [hep-th]].
- [31] J. Knapp, M. Kreuzer, C. Mayrhofer and N. O. Walliser, JHEP **1103** (2011) 138 [arXiv:1101.4908 [hep-th]].
- [32] M. J. Dolan, J. Marsano, N. Saulina and S. Schafer-Nameki, Phys. Rev. D **84** (2011) 066008 [arXiv:1102.0290 [hep-th]].
- [33] J. Marsano and S. SchaferNameki, JHEP **1111** (2011) 098 [arXiv:1108.1794 [hep-th]].
- [34] T. W. Grimm, M. Kerstan, E. Palti and T. Weigand, JHEP **1112** (2011) 004 [arXiv:1107.3842 [hep-th]].
- [35] D. R. Morrison and D. S. Park, JHEP **1210** (2012) 128 [arXiv:1208.2695 [hep-th]].
- [36] C. Mayrhofer, E. Palti and T. Weigand, JHEP **1303** (2013) 098 [arXiv:1211.6742 [hep-th]].
- [37] V. Braun, T. W. Grimm and J. Keitel, JHEP **1309** (2013) 154 [arXiv:1302.1854 [hep-th]].
- [38] J. Borchmann, C. Mayrhofer, E. Palti and T. Weigand, Phys. Rev. D **88** (2013) no.4, 046005 [arXiv:1303.5054 [hep-th]].
- [39] M. Cvetič, D. Klevers and H. Piragua, JHEP **1306** (2013) 067 [arXiv:1303.6970 [hep-th]].
- [40] V. Braun, T. W. Grimm and J. Keitel, JHEP **1312** (2013) 069 [arXiv:1306.0577 [hep-th]].
- [41] M. Cvetič, A. Grassi, D. Klevers and H. Piragua, JHEP **1404** (2014) 010 [arXiv:1306.3987 [hep-th]].
- [42] M. Cvetič, D. Klevers and H. Piragua, JHEP **1312** (2013) 056 [arXiv:1307.6425 [hep-th]].
- [43] J. Borchmann, C. Mayrhofer, E. Palti and T. Weigand, Nucl. Phys. B **882** (2014) 1 [arXiv:1307.2902 [hep-th]].
- [44] M. Cvetič, D. Klevers, H. Piragua and P. Song, JHEP **1403** (2014) 021 [arXiv:1310.0463 [hep-th]].
- [45] I. Antoniadis and G. K. Leontaris, Phys. Lett. B **735** (2014) 226 [arXiv:1404.6720 [hep-th]].
- [46] C. Lawrie, S. Schafer-Nameki and J. M. Wong, JHEP **1509** (2015) 144 [arXiv:1504.05593 [hep-th]].
- [47] M. Cvetič, D. Klevers, H. Piragua and W. Taylor, JHEP **1511** (2015) 204 [arXiv:1507.05954 [hep-th]].
- [48] M. Cvetič, A. Grassi, D. Klevers, M. Poretschkin and P. Song, JHEP **1604** (2016) 041 [arXiv:1511.08208 [hep-th]].
- [49] Y. Kimura and S. Mizoguchi, PTEP **2018** (2018) no.4, 043B05 [arXiv:1712.08539 [hep-th]].

- [50] Y. Kimura, JHEP **1805**, 048 (2018) [arXiv:1802.05195 [hep-th]].
- [51] M.R. Gaberdiel, T. Hauer and B. Zwiebach, Open string - string junction transitions, Nucl. Phys. B525 (1998) 117, hep-th/9801205.
- [52] O. DeWolfe and B. Zwiebach, String Junctions for Arbitrary Lie Algebra Representations, Nucl. Phys. B541 (1999) 509, hep-th/9804210.
- [53] O. DeWolfe, T. Hauer, A. Iqbal and B. Zwiebach, Uncovering the Symmetries on $[p, q]$ 7-branes: Beyond the Kodaira Classification, hep-th/9812028.
- [54] J. H. Schwarz, Phys. Lett. B **360** (1995) 13 Erratum: [Phys. Lett. B **364** (1995) 252] [hep-th/9508143].
- [55] T. Tani, Nucl. Phys. B **602** (2001) 434.
- [56] L. Bonora and R. Savelli, JHEP **1011** (2010) 025 [arXiv:1007.4668 [hep-th]].
- [57] M. Fukae, Y. Yamada and S-K. Yang, Nucl.Phys.B572(2000)71-94.
- [58] A. Grassi, J. Halverson and J. L. Shaneson, JHEP **1310** (2013) 205 [arXiv:1306.1832 [hep-th]].
- [59] A. Grassi, J. Halverson and J. L. Shaneson, Commun. Math. Phys. **336** (2015) no.3, 1231 [arXiv:1402.5962 [hep-th]].
- [60] A. Grothendieck, "Esquisse d'un Programme", (1984 manuscript). Published in Schneps and Lochak (1997, I), pp.5-48; English transl., *ibid.*, pp. 243-283. MR1483107.
- [61] S.K.Lando and A.K.Zvonkin, "Graphs on Surfaces and Their Applications, Encyclopaedia of Mathematical Sciences: Lower-Dimensional Topology II", 141, (2004). Berlin, New York: Springer-Verlag, ISBN 978-3-540-00203-1, Zbl 1040.05001.
- [62] N. Seiberg and E. Witten, Nucl. Phys. B **431** (1994) 484 [hep-th/9408099].
- [63] A. Sen, Nucl. Phys. B **475** (1996) 562 [hep-th/9605150].
- [64] M. Bershadsky, K. A. Intriligator, S. Kachru, D. R. Morrison, V. Sadov and C. Vafa, Nucl. Phys. B **481** (1996) 215 [hep-th/9605200].
- [65] D. R. Morrison and W. Taylor, JHEP **1201**, 022 (2012) [arXiv:1106.3563 [hep-th]].
- [66] S. Mizoguchi, JHEP **1407** (2014) 018 [arXiv:1403.7066 [hep-th]].
- [67] S. Mizoguchi and T. Tani, PTEP **2016** (2016) no.7, 073B05 [arXiv:1508.07423 [hep-th]].